

BIPOLARON BINDING IN QUANTUM WIRES

E. P. Pokatilov

*Laboratory Physics of Multilayer Structures, Department of Theoretical Physics,
State University of Moldova, str. A. Mateevici, 60, MD-2009 Kishinev, Republic of Moldova*

V. M. Fomin^a, J. T. Devreese^b

*Theoretische Fysica van de Vaste Stof, Departement Natuurkunde,
Universiteit Antwerpen (U.I.A.), Universiteitsplein 1, B-2610 Antwerpen, Belgium*

S. N. Balaban, and S. N. Klimin^c

*Laboratory Physics of Multilayer Structures, Department of Theoretical Physics,
State University of Moldova, str. A. Mateevici, 60, MD-2009 Kishinev, Republic of Moldova*

Phys. Rev. B **61**, 2721-2728 (2000) ©2000 The American Physical Society

Abstract

A theory of bipolaron states in quantum wires with a parabolic potential well is developed applying the Feynman variational principle. The basic parameters of the bipolaron ground state (the binding energy, the number of phonons in the bipolaron cloud, the effective mass, and the bipolaron radius) are studied as a function of sizes of the potential well. Two cases are considered in detail: a cylindrical quantum wire and a planar quantum wire. Analytical expressions for the bipolaron parameters are obtained at large and small sizes of the quantum well. It is shown that at $R \gg 1$ [where R means the radius (halfwidth) of a cylindrical (planar) quantum wire, expressed in Feynman units], the influence of confinement on the bipolaron binding energy is described by the function $\sim 1/R^2$ for both cases, while at small sizes this influence is different in each case. In quantum wires, the bipolaron binding energy $W(R)$ increases logarithmically with decreasing radius. The shapes and the sizes of a nanostructure, which are favorable for observation of stable bipolaron states, are determined.

I. INTRODUCTION

Landau's idea [1] of the auto-localized state of a charge carrier (polaron) in a homogeneous polar medium got a further development by Pekar [2] who first studied a problem of a stable complex of two charge carriers of the same sign (bipolaron). The bipolaron binding energy was first calculated in Ref. [3]. The bipolaron problem was widely discussed, see e. g. Refs. [4–9]. A detailed outline of this subject is presented in the recent review [10].

Dimensionless constants of the Coulomb interaction U and of the electron-phonon interaction α are related to each other by the equation [10]:

$$U = \frac{\sqrt{2}\alpha}{1 - \eta}, \quad (1)$$

where $\eta = \varepsilon_\infty/\varepsilon_0$ (ε_0 and ε_∞ are static and optical dielectric constants, respectively). Due to the fact that $\varepsilon_0 > \varepsilon_\infty$, the relation $U \geq \sqrt{2}\alpha$ follows. When the distance l between electrons is large or small compared with the characteristic polaron radius R_p (see Ref. [11]), the phonon-mediated attraction between electrons occurs to be weaker than the repulsion. At large distances $l \gg R_p$, both interaction potentials have similar spatial dependences but the Coulomb repulsion is stronger than the phonon-mediated attraction. In the opposite case, $l \ll R_p$, the Coulomb potential diverges at the zero distance, while the phonon-mediated attraction is always finite. Nevertheless, when two electrons move in such a way that the average distance between them is of the same order as the polaron radius, the bipolaron can be stable at $\alpha \gg 1$ and $\eta \ll 1$. When two electrons are together confined to a potential well, one can expect that the conditions of the bipolaron stability may be improved for relevant sizes of the well.

Two new circumstances have stimulated the bipolaron theory: the progress in the fabrication technology of mesoscopic nanostructures such as quasi-2D (quantum wells and superlattices), quasi-1D (quantum wires), quasi-0D (quantum dots), and the advancement of the hypothesis that bipolaron excitations might play a role in processes occurring in the high-temperature superconductors. The present research has been motivated also by the recent advances in creation of nanocrystals with a strong ionic coupling [12].

The basic bipolaron parameters are recalled in what follows. The bipolaron stability region is determined by the inequality $W > 0$ for the bipolaron binding energy

$$W \equiv 2E_p - E_{\text{bip}}. \quad (2)$$

Here E_p and E_{bip} are the free polaron and bipolaron ground state energies, respectively. From the equation

$$W(\alpha, \eta, \mathcal{R}) = 0, \quad (3)$$

where \mathcal{R} denotes the set of parameters determining the shape and the size of the confinement domain, the functions $\alpha_c(\eta, \mathcal{R})$ and $\eta_c(\alpha, \mathcal{R})$ describing the boundaries of the bipolaron stability region are found, for fixed η and α , respectively. According to different theoretical treatments [4–10] the bipolaron binding energy is an increasing function of α and a decreasing function of η . It will be shown that the function $\eta_c(\alpha, \mathcal{R})$ starts from $\eta_c = 0$ at $\alpha = \alpha_{\text{min}}(\mathcal{R}) \neq 0$, grows with increasing α and tends to the upper limit η_{max} at $\alpha \rightarrow \infty$. The bipolaron stability region is then determined by the inequalities $\alpha \geq \alpha_{\text{min}}(\mathcal{R})$ and $0 \leq \eta < \eta_c(\alpha, \mathcal{R})$.

Let us adduce typical values of the parameters $\alpha_{\text{min},3\text{D}}$ and $\eta_{\text{max},3\text{D}}$ of the bulk (3D) bipolaron: $\alpha_{\text{min},3\text{D}} = 6.8$ and $\eta_{\text{max},3\text{D}} = 0.14$ were found by Verbist, Peeters and Devreese [13,14] and by Verbist, Smondyrev, Peeters and Devreese [15]. Adamowski [7] obtained $\alpha_{\text{min},3\text{D}} = 7.3$ and $\eta_{\text{max},3\text{D}} = 0.14$. The bipolaron theory developed for pure 2D [16,17] and 1D [17] models shows that the bipolaron stability region broadens when the dimensionality

is reduced. For these systems, the following parameters were obtained: $\alpha_{\min,2D} = 2.9$, $\eta_{\max,2D} = 0.158$ (Ref. [16]); $\alpha_{\min,1D} = 0.9$, $\eta_{\max,1D} = 0.764$ (Ref. [18]). Bipolaron states were investigated in a quantum well [19,20] and in a quantum wire [21] as a function of the characteristic size of the system. The polaron theory for a quantum dot is developed in Refs. [22–25].

The goal of the present investigation is to determine the bipolaron stability region and to study the basic parameters characterizing the bipolaron ground state as a function of confinement. Two different types of confinement are considered and compared to each other: (i) a cylindrical quantum wire of the radius R , where continuous transitions from 3D to 1D are realized with decreasing R ; (ii) a planar quantum wire of the width L , where a transition from 2D to 1D is realized with decreasing L . A unique approach, namely the Feynman variational method [26,27], is used throughout the paper for both systems under analysis.

The paper is organized as follows. In Section II, general formulae for parameters of a bipolaron in quantum wires are deduced. In Section III, particular cases of cylindrical and planar quantum wires are considered. The basic parameters of the bipolaron ground state are obtained. Limiting cases of strong and weak confinement are studied in detail. The obtained numerical and analytical results are discussed in Section IV. Section V contains conclusions about the influence of confinement on the bipolaron binding energy in quantum wires.

II. GENERAL THEORY

We analyze the bipolaron problem taking into account both the electron-phonon interaction and the Coulomb repulsion between two electrons confined to a quantum wire. The Lagrange function of the system is

$$L = \sum_{i=1}^D \sum_{n=1,2} \frac{m_i \dot{x}_{i,n}^2}{2} - \sum_{n=1,2} \mathcal{U}(\mathbf{r}_n) - \frac{e^2}{\varepsilon_\infty |\mathbf{r}_1 - \mathbf{r}_2|} + \frac{1}{2} \sum_{\mathbf{k}} \left(\dot{w}_{\mathbf{k}}^2 - \omega_0^2 w_{\mathbf{k}}^2 \right) - \sum_{n=1,2} \sum_{\mathbf{k}} \gamma_{\mathbf{k}}(\mathbf{r}_n) w_{\mathbf{k}}, \quad (4)$$

where $\mathbf{r}_n (x_{1n}, x_{2n}, x_{3n})$ is the radius vector of the n -th electron ($n = 1, 2$); m_i is the ii -th component ($i = 1, 2, 3$) of the diagonal band mass tensor, $\mathcal{U}(\mathbf{r})$ is the potential energy of an electron in the quantum wire, $w_{\mathbf{k}}$ are the normal coordinates of longitudinal optical (LO) phonon modes. Here, the parameter D determines the dimensionality of the electron subsystem: $D = 3$ and 2 for cylindrical and planar quantum wires, respectively. Amplitudes of the electron-phonon interaction are taken in the Fröhlich form:

$$\gamma_{\mathbf{k}}(\mathbf{r}) = 2\sqrt{\frac{2\pi\hbar\omega_0\alpha\omega_0}{V} \frac{\omega_0}{k}} \left(\frac{\hbar}{2\bar{m}\omega_0} \right)^{1/4} \exp(i\mathbf{k}\mathbf{r}), \quad (5)$$

where $\bar{m} \equiv (m_1 m_2 m_3)^{1/3}$, V is the volume of the system, and the Fröhlich constant

$$\alpha = \frac{e^2}{2\hbar\omega_0} \left(\frac{1}{\varepsilon_\infty} - \frac{1}{\varepsilon_0} \right) \left(\frac{2\bar{m}\omega_0}{\hbar} \right)^{1/2} \quad (6)$$

characterizes the strength of the coupling between an electron and bulk polar LO phonons with the long-wavelength frequency ω_0 . In this paper, the 3D phonon approximation is used, according to which the interaction of an electron with both bulk-like and interface phonons is replaced by that with 3D phonons. This often used approach is adequate because any integral polaron or bipolaron effect, resulting from a summation over all phonon modes, appears to be only weakly dependent on the details of the phonon spectrum. It should be also mentioned that the system under consideration simulates realistic structures with relatively smooth interface barriers, where interface-like phonon modes can appear, which are smoothly distributed in space rather than localized near a sharp boundary, as is the case for interface modes.

In order to study the bipolaron problem at arbitrary values of α , the Feynman variational approach [27] is the most appropriate method. The trial Lagrange function is written as

$$L_{tr} = \frac{1}{2} \sum_{i=1}^D \sum_{n=1,2} \left[m_i \dot{x}_{i,n}^2 + M_i \dot{X}_{i,n}^2 - k_i (x_{i,n} - X_{i,n})^2 - k'_i (x_{i,n} - X_{i,\bar{n}})^2 \right] + \sum_{i=1}^3 K_i (x_{i1} - x_{i2})^2 - \sum_{n=1,2} \mathcal{W}(\mathbf{r}_n), \quad (7)$$

where X_{in} are coordinates of the n -th “fictitious” particle ($n = 1, 2$). This model imitates the interaction of electrons with phonons and between each other by elastic bonds as shown in Fig. 1. The masses M_i and the force constants k_i, k'_i, K_i play the role of variational parameters. For $n = 1$, \bar{n} takes the value 2, and for $n = 2$, \bar{n} is equal to 1. The potential well $\mathcal{U}(\mathbf{r})$ from Eq. (4) is simulated here by a parabolic function:

$$\mathcal{W}(\mathbf{r}) = \frac{1}{2} \sum_{i=1}^q m_i \Omega_i^2 x_i^2. \quad (8)$$

The index q characterizes the dimensionality of confinement and is determined as follows: for a planar quantum wire $q = 1$ ($\Omega_1 \neq 0$ and $\Omega_2 = 0$) and for a cylindrical quantum wire $q = 2$ ($\Omega_1 \neq 0, \Omega_2 \neq 0$, and $\Omega_3 = 0$).

The basis of the Feynman variational method is the Jensen-Feynman inequality [27]:

$$\langle \exp(S - S_{tr}) \rangle_{S_{tr}} \geq \exp \langle S - S_{tr} \rangle_{S_{tr}}, \quad (9)$$

where the angular brackets denote averaging over electron paths:

$$\langle G \rangle_{S_{tr}} = \frac{\text{Tr} \int D\mathbf{r} G[\mathbf{r}] \exp(S_{tr})}{\text{Tr} \int D\mathbf{r} \exp(S_{tr})}. \quad (10)$$

Here S and S_{tr} are the electron action functionals obtained after integration over phonon variables and over coordinates of “fictitious” particles, respectively. At low temperatures, the variational bipolaron energy is calculated using the expression

$$E_{bip} = E_{tr} - \lim_{\beta \rightarrow \infty} \frac{\langle S - S_{tr} \rangle_{S_{tr}}}{\beta}, \quad (11)$$

where E_{tr} is the ground state energy of the trial system with the Lagrangian (7), $\beta = 1/k_B T$ is the inverse temperature.

The trial Lagrange function (7) consists of D independent parts: $L_{tr} = \sum_{i=1}^D L_i$. Each part L_i is a function of four variables $x_{i1}, x_{i2}, X_{i1}, X_{i2}$. Let us introduce unified denotations for coordinates of electrons and of “fictitious” particles: $\tilde{x}_{i1} = x_{i1}, \tilde{x}_{i2} = x_{i2}, \tilde{x}_{i3} = X_{i1}, \tilde{x}_{i4} = X_{i2}$. It follows from the form of the trial Lagrangian (7) with Eq. (8) that the groups of variables \tilde{x}_{ij} with different indices i are dynamically independent from each other. They are related to normal variables ξ_{ij} by the unitary transformation:

$$\tilde{x}_{ij} = \sum_{j'=1}^4 d_{i,jj'} \xi_{ij'}, \quad i = 1, \dots, D \quad (12)$$

with 4×4 matrices $\|d_{i,jj'}\|$ ($j, j' = 1, \dots, 4$). From the equations of motion for the group of coordinates \tilde{x}_{ij} ($j = 1, \dots, 4$) with a fixed i , the following eigenfrequencies are obtained:

$$\begin{aligned} \omega_{ij}^2 &= \frac{1}{2} \left\{ \left(1 + \frac{M_i}{m_i}\right) v_i^2 + \Omega_i^2 - (-1)^j \sqrt{\left[\left(1 - \frac{M_i}{m_i}\right) v_i^2 - \Omega_i^2\right]^2 + 4 \frac{M_i}{m_i} v_i^4} \right\}, \quad j = 1, 2, \\ \omega_{ij}^2 &= \frac{1}{2} \left\{ \left(1 + \frac{M_i}{m_i}\right) v_i^2 + \Omega_i^2 - 2 \frac{K_i}{m_i} - (-1)^j \sqrt{\left[\left(1 - \frac{M_i}{m_i}\right) v_i^2 - \Omega_i^2 + 2 \frac{K_i}{m_i}\right]^2 + 4 \frac{(k_i - k'_i)^2}{m_i M_i}} \right\}, \\ & \hspace{20em} j = 3, 4, \end{aligned} \quad (13)$$

where $v_i^2 = (k_i + k'_i)/M_i$. Matrix elements of the unitary transformation (12) are

$$\begin{aligned} d_{i,11}^2 &= \frac{\omega_{i1}^2 - v_i^2}{2(\omega_{i1}^2 - \omega_{i2}^2)}, \quad d_{i,12}^2 = \frac{v_i^2 - \omega_{i2}^2}{2(\omega_{i1}^2 - \omega_{i2}^2)}, \quad d_{i,13}^2 = \frac{\omega_{i3}^2 - v_i^2}{2(\omega_{i3}^2 - \omega_{i4}^2)}, \quad d_{i,14}^2 = \frac{v_i^2 - \omega_{i4}^2}{2(\omega_{i3}^2 - \omega_{i4}^2)}, \\ d_{i,2j'} &= s_{j'} d_{i,1j'}; \quad d_{i,3j'} = \frac{k_i + s_{j'} k'_i}{M_i (v_i^2 - \omega_{ij'}^2)} d_{i,1j'}; \quad d_{i,4j'} = s_{j'} d_{i,3j'}; \end{aligned} \quad (14)$$

$$s_j = 1 \quad (j = 1, 2); \quad s_j = -1 \quad (j = 3, 4).$$

Note that the elastic repulsion imitating the Coulomb interaction gives a contribution to the eigenfrequencies with $j = 3$ and 4 through the force constants K_i . It is easy to see from Eq. (13) that under the conditions of a strong confinement along the i -th coordinate axis the eigenfrequencies with $j = 1$ and 3 corresponding to the motion of the bipolaron along this axis as a whole are determined mainly by the parameter Ω_i .

The action functionals S and S_{tr} in Eqs. (9) to (11) contain the potential energies \mathcal{U} and \mathcal{W} , respectively. Though the shape of a real potential \mathcal{U} may differ from that of the model quadratic potential (8), the averaged difference $\langle \mathcal{U} - \mathcal{W} \rangle_{S_{tr}}$ can be omitted as far as it is small when compared to the rest of $\langle S - S_{tr} \rangle_{S_{tr}} / \beta$.

The averaging procedure in Eq. (11) is carried out by the path integration and leads to the following form of the variational bipolaron energy:

$$E_{\text{bip}} = \sum_{i=1}^D B_i + C + P. \quad (15)$$

Here the terms B_i include the averaged kinetic energies of two electrons and of two “fictitious” particles as well as the averaged potential energy of the elastic interaction of these four particles:

$$B_i = \frac{1}{2} \sum_{j=1}^4 \omega_{ij} \left(1 - \frac{\omega_{ij}^2 - \Omega_i^2}{\omega_{ij}^2} d_{i,1j}^2 \right) - v_i, \quad i = 1, \dots, D. \quad (16)$$

In Eqs. (15), (16) and further on, the Feynman units [26] are used: $\hbar\omega_0$ for energies; ω_0 for frequencies; and $(\hbar/\bar{m}\omega_0)^{1/2}$ for lengths.

The averaged potential energy of the Coulomb electron repulsion is

$$C = \frac{\alpha}{(1-\eta)\pi^2} \mathcal{K}_2(0), \quad (17)$$

and the averaged energy of the electron-phonon interaction is

$$P = -\frac{\alpha}{\pi^2} \sum_{n=1,2} \int_0^\infty d\tau e^{-\tau} \mathcal{K}_n(\tau), \quad (18)$$

where

$$\mathcal{K}_n(\tau) = \int_{-\infty}^\infty \frac{1}{k^2} \exp \left[-\sum_{i=1}^D k_i^2 A_{in}(\tau) \right] \prod_{i=1}^D dk_i. \quad (19)$$

The functions $A_{in}(\tau)$ are determined as follows:

$$A_{in}(\tau) = \frac{\bar{m}}{m_i} \left[\sum_{j=1,2} \frac{d_{i,1j}^2}{\omega_{ij}} (1 - e^{-\omega_{ij}\tau}) + \sum_{j=3,4} \frac{d_{i,1j}^2}{\omega_{ij}} (1 + (-1)^n e^{-\omega_{ij}\tau}) \right], \quad n = 1, 2. \quad (20)$$

In order to find the bipolaron energy, it is necessary to minimize the function E_{bip} given by Eq. (15) over twelve independent variational parameters ω_{ij} , $i = 1 \dots 3$, $j = 1 \dots 4$, which are used instead of the masses M_i and the force constants k_i , k'_i , K_i .

From Eq. (13) for the eigenfrequencies, the expression for components of the diagonal tensor of relative bipolaron effective mass is deduced straightforwardly:

$$\frac{(m_{\text{bip}})_i}{m_i} \equiv 2 \left(\frac{M_i}{m_i} + 1 \right) = \frac{2(\omega_{i1}^2 + \omega_{i2}^2 - \Omega_i^2)}{v_i^2}, \quad (21)$$

where the values of parameters ω_{i1} , ω_{i2} , v_i are taken which provide the bipolaron energy.

The number of phonons in the bipolaron cloud is determined by the general expression of Ref. [11]

$$N_{\text{ph}} = \left\langle \frac{\partial S}{\partial (\hbar\omega_0)} \right\rangle_{S_{tr}}, \quad (22)$$

which gives in the case under consideration:

$$N_{\text{ph}} = \frac{\alpha}{\pi^2} \sum_{n=1,2} \int_0^\infty \mathcal{K}_n(\tau) e^{-\tau} \tau d\tau. \quad (23)$$

Calculations of the average number of phonons according to Eq. (23) are performed using the results of minimization of the bipolaron energy.

III. BIPOLARON IN CYLINDRICAL AND PLANAR QUANTUM WIRES

A. Variational problem

Here we write down the variational bipolaron energies in the cylindrical and planar quantum wires (see Fig. 2). Hereafter, the following denotation for the confinement parameter is used: $\Omega_i \equiv \Omega_{\perp}$, $i = 1, q$. The electron mass is taken to be isotropic, i. e. $m_1 = m_2 = m_3 = m$. From Eqs. (15) to (18) we obtain the variational bipolaron energy

$$E_{\text{bip}} = B_{\perp} + B_{\parallel} + C + P, \quad (24)$$

where, in accordance with Eq. (16),

$$B_{\parallel} = \frac{1}{2} \sum_{j=1}^3 \omega_{\parallel j} \left(1 - d_{\text{D},1j}^2 \right) - v_{\parallel}, \quad (25)$$

$$B_{\perp} = \frac{q}{2} \left[\sum_{j=1}^4 \omega_{\perp j} \left(1 - \frac{\omega_{\perp j}^2 - \Omega_{\perp}^2}{\omega_{\perp j}^2} d_{1,1j}^2 \right) - 2v_{\perp} \right]. \quad (26)$$

Here the frequencies of the motion along the z -axis (called below the longitudinal motion) are

$$\omega_{\text{D}1} \equiv \omega_{\parallel 1} \quad \omega_{\text{D}2} = 0, \quad \omega_{\text{D}j} \equiv \omega_{\parallel j}, \quad j = 3, 4, \quad (27)$$

$$v_{\text{D}} \equiv v_{\parallel}$$

and those of the motion in the xy -plane (the transverse motion) are

$$\omega_{ij} \equiv \omega_{\perp j}, \quad j = 1, \dots, 4, \quad v_i \equiv v_{\perp} \quad (28)$$

with $i = 1, 2$ for $q = 2$ and $i = 1$ for $q = 1$. In the case under consideration, the integrations containing the function $\mathcal{K}_n(\tau)$ are performed analytically. The calculation of the integrals in Eqs. (17) and (18) yields the averaged potential energy of the Coulomb repulsion between electrons

$$C = \frac{\sqrt{2}U}{\sqrt{\pi}A_{\parallel 2}(0)} F_q \left(1 - \frac{A_{\perp 2}(0)}{A_{\parallel 2}(0)} \right) \quad (29)$$

and the averaged energy of the electron-phonon interaction

$$P = -\frac{2\alpha}{\sqrt{\pi}} \sum_{n=1,2} \int_0^{\infty} d\tau e^{-\tau} \frac{1}{\sqrt{A_{\parallel n}(\tau)}} F_q \left(1 - \frac{A_{\perp n}(\tau)}{A_{\parallel n}(\tau)} \right), \quad (30)$$

where

$$A_{\parallel n}(\tau) = \sum_{j=3,4} \frac{d_{\text{D},1j}^2}{\omega_{\parallel j}} \left[1 + (-1)^n e^{-\omega_{\parallel j}\tau} \right] + \frac{d_{\text{D},11}^2}{\omega_{\parallel 1}} \left(1 - e^{-\omega_{\parallel 1}\tau} \right) + d_{\text{D},12}^2 \tau;$$

$$A_{\perp n}(\tau) = \sum_{j=1,2} \frac{d_{1,1j}^2}{\omega_{\perp j}} \left(1 - e^{-\omega_{\perp j}\tau}\right) + \sum_{j=3,4} \frac{d_{1,1j}^2}{\omega_{\perp j}} \left[1 + (-1)^n e^{-\omega_{\perp j}\tau}\right], \quad n = 1, 2;$$

$$F_q(x) = \begin{cases} \frac{\tanh^{-1}\sqrt{x}}{\sqrt{x}}, & q = 2; \\ \int_0^{\frac{\pi}{2}} \frac{d\varphi}{(1-x\sin^2\varphi)^{1/2}}, & q = 1. \end{cases} \quad (31)$$

The minimization of the variational bipolaron energy E_{bip} determined by Eqs. (24) to (31) is carried out with respect to eight variational parameters v_{\parallel} , $\omega_{\perp 2}$, $\omega_{\parallel j}$, $\omega_{\perp j}$ ($j = 1, 3, 4$). Setting k'_i and K_i equal to zero in these formulas, the twice value of the polaron energy [25] is obtained from Eq. (24). The binding energy is then found according to Eq. (2). Results of the calculation of W as a function of the quantum wire radius $R = \Omega_{\perp}^{-1/2}$ are presented in Fig. 3 for different values of α . Then the functions $\alpha_{\text{min}}(R) \equiv \alpha_c(\eta = 0, R)$ (Fig. 4) and $\eta_c(R, \alpha)$ are obtained. The latter function is used for calculation of the critical value of the Coulomb repulsion constant $U_c(\alpha)$ in order to describe the bipolaron stability region shown in Fig. 5. From Eq. (21), taking into account Eq. (27), the relative bipolaron effective mass of the longitudinal motion is derived as

$$\frac{(m_{\text{bip}})_{\parallel}}{m} = \frac{2\omega_{\parallel 1}^2}{v_{\parallel}^2}. \quad (32)$$

Plots of the relative bipolaron mass as a function of R are shown in Fig. 6. A detailed discussion of the results will be given in Section IV.

B. Weak size quantization

For a weak size quantization, the eigenfrequencies of the transverse motion can be represented as expansion series in Ω_{\perp} . In these series, we take into account only two first terms:

$$\begin{aligned} \omega_{\perp 1}^2 &= \omega_{\parallel 1}^2 + \Omega_{\perp}^2 \frac{\omega_{\parallel 1}^2 - v_{\parallel}^2}{\omega_{\parallel 1}^2} + O(\Omega_{\perp}^4), & \omega_{\perp 2}^2 &= \Omega_{\perp}^2 \frac{v_{\parallel}^2}{\omega_{\parallel 1}^2} + O(\Omega_{\perp}^4), \\ \omega_{\perp 3}^2 &= \omega_{\parallel 3}^2 + \Omega_{\perp}^2 \frac{\omega_{\parallel 3}^2 - v_{\parallel}^2}{\omega_{\parallel 3}^2 - \omega_{\parallel 4}^2} + O(\Omega_{\perp}^4), & \omega_{\perp 4}^2 &= \omega_{\parallel 4}^2 + \Omega_{\perp}^2 \frac{v_{\parallel}^2 - \omega_{\parallel 4}^2}{\omega_{\parallel 3}^2 - \omega_{\parallel 4}^2} + O(\Omega_{\perp}^4). \end{aligned} \quad (33)$$

As a consequence, Eq. (26) takes on the form

$$B_{\perp} = q \left[B_{\parallel} + \Omega_{\perp} \frac{v_{\parallel}}{4\omega_{\parallel 1}} \frac{3\omega_{\parallel 1}^2 - v_{\parallel}^2}{\omega_{\parallel 1}^2} \right] + O(\Omega_{\perp}^2), \quad (34)$$

and the parameters in the right-hand side of Eq. (30) satisfy the relations

$$A_{\perp n}(\tau) = A_{\parallel n}(\tau) - \frac{1}{4} \Omega_{\perp} \tau^2 \frac{v_{\parallel}^3}{\omega_{\parallel 1}^3} + O(\Omega_{\perp}^2), \quad n = 1, 2. \quad (35)$$

Substituting the expression (35) in Eqs. (29), (30), we obtain the energy of the Coulomb repulsion

$$C = \frac{\sqrt{2}U}{\sqrt{\pi}} \frac{f_{1q}}{\sqrt{A_{\parallel 12}(0)}} + O(\Omega_{\perp}^2), \quad (36)$$

and the energy of the electron-phonon interaction

$$P = -\frac{2\alpha}{\sqrt{\pi}} \sum_{n=1,2} \int_0^{\infty} d\tau e^{-\tau} \left[\frac{f_{1q}}{\sqrt{A_{\parallel n}(\tau)}} + \frac{\Omega_{\perp}}{4} \tau^2 \frac{v_{\parallel}^3}{\omega_{\parallel 1}^3} \frac{f_{2q}}{\sqrt{A_{\parallel n}^3(\tau)}} \right] + O(\Omega_{\perp}^2), \quad (37)$$

where

$$f_{1q} = \begin{cases} 1, & q = 2; \\ \frac{\pi}{2}, & q = 1, \end{cases} \quad f_{2q} = \begin{cases} \frac{1}{3}, & q = 2; \\ \frac{\pi}{8}, & q = 1. \end{cases}$$

The bipolaron energy in this limiting case can be represented as

$$E_{\text{bip}} = E_{\text{bip}}^0 + \Delta E_{\text{bip}} + O(\Omega_{\perp}^2),$$

where E_{bip}^0 is the bipolaron energy in three or two dimensions for $D = 3$ or $D = 2$, respectively. The confinement-induced shift of the bipolaron energy ΔE_{bip} is given by

$$\Delta E_{\text{bip}} = \Omega_{\perp} \left\{ q \frac{v_{\parallel}}{4\omega_3} \frac{3\omega_{\parallel 1}^2 - v_{\parallel}^2}{\omega_{\parallel 1}^2} - \frac{2\alpha}{\sqrt{\pi}} f_{2q} \frac{v_{\parallel}^3}{4\omega_{\parallel 1}^2} \int_0^{\infty} d\tau e^{-\tau} \tau^2 \left(\frac{1}{\sqrt{A_{\parallel 11}^3(\tau)}} + \frac{1}{\sqrt{A_{\parallel 12}^3(\tau)}} \right) \right\}. \quad (38)$$

It is worth mentioning, that in the strong coupling regime, the integrals in Eq. (38) are calculated analytically, and the minimization of this variational function with respect to the frequencies is performed explicitly. For this purpose we use the results of Ref. [28], where the following analytical expressions for frequencies are obtained: $\omega_{\parallel i} = \alpha^2 \tilde{\omega}_i$ (for $i = 1, 3$), $\omega_{\parallel 4} = 1, v_{\parallel} = 1$, where

$$\tilde{\omega}_1 = \frac{128}{9\pi} \theta_D \frac{[1 - \zeta^2(U)]^4}{\zeta^2(U)}, \quad \tilde{\omega}_3 = \frac{128}{9\pi} \theta_D [1 - \zeta^2(U)]^3, \quad (39)$$

$$\zeta(U) = \frac{U}{16\alpha} + \frac{1}{2} \sqrt{2 + \left(\frac{U}{8\alpha}\right)^2}, \quad \theta_D = \begin{cases} 1, & D = 3; \\ \left(\frac{3\pi}{4}\right)^2, & D = 2. \end{cases}$$

Using these frequencies, we find the confinement-induced shift of the bipolaron energy to be

$$\Delta E_{\text{bip}} = q \frac{\Omega_{\perp}}{2\alpha^2 \tilde{\omega}_3}. \quad (40)$$

This result differs qualitatively from that deduced in Ref. [29] for a bipolaron in a weak magnetic field, where the cyclotron frequency ω_c plays the role of Ω . Namely, as distinct from Eq. (40), in the equation from Ref. [29] for the first-order correction to the bipolaron energy α^2 stands instead of α^4 .

It is important to note, that this positive correction to the bipolaron energy due to the confinement is less than the twice value of the respective correction to the polaron energy [25]. The confinement-induced variation of the bipolaron binding energy obeys the inequality

$$\Delta W = \frac{q}{2} \frac{\Omega}{\alpha^2} \left[\frac{9\pi}{2\theta_D} - \frac{1}{\tilde{\omega}_3} \right] > 0. \quad (41)$$

Thus, the enhancement of the bipolaron binding takes place due to the confinement.

C. Strong size quantization

In the limiting case of a strong size quantization, the terms of the order of Ω_{\perp}^2 play a determining role in Eq. (15). For the frequencies of the transverse motion, the expansion in inverse powers of Ω^2 gives:

$$\begin{aligned}\omega_{\perp 1}^2 &= \Omega_{\perp}^2 + \frac{M_1}{m} v_{\perp}^2 + O(\Omega_{\perp}^{-2}), & \omega_{\perp 2}^2 &= v_{\perp}^2 + O(\Omega_{\perp}^{-2}), \\ \omega_{\perp 3}^2 &= \Omega_{\perp}^2 + \frac{M_1}{m} v_{\perp}^2 - 2\frac{K_{\perp}}{m} + O(\Omega_{\perp}^{-2}), & \omega_{\perp 4}^2 &= v_{\perp}^2 + O(\Omega_{\perp}^{-2}).\end{aligned}\quad (42)$$

Consequently, the bipolaron ground state energy is described by the expression

$$\begin{aligned}E_{\text{bip}} &= q\Omega_{\perp} + T_{\parallel} + \frac{U}{\sqrt{2\pi A_{\parallel 2}(0)}} \ln \left(\frac{16}{q^2} \Omega_{\perp} A_{\parallel 2}(0) \right) \\ &\quad - \frac{\alpha}{\sqrt{\pi}} \sum_{n=1,2} \int_0^{\infty} d\tau e^{-\tau} \frac{1}{\sqrt{A_{\parallel n}(\tau)}} \ln \left(\frac{16}{q^2} \Omega_{\perp} A_{\parallel n}(\tau) \right).\end{aligned}\quad (43)$$

The first term in the right-hand side of Eq. (43) is the energy of two electrons in the parabolic potential. The last three terms in the right-hand side of Eq. (43) are due to the electron-phonon and Coulomb interactions. In the strong coupling regime, $\omega_{\parallel i} = \alpha^2 \tilde{\omega}_i$ ($i = 1, 3$); $\omega_{\parallel 4}$ and v_{\parallel} are proportional to α^0 with coefficients which are functions of Ω_{\perp} . Then omitting the terms of the order of α^0 in the last three terms of the variational bipolaron energy (43) we obtain

$$\begin{aligned}E_{\text{bip}} &= q\Omega_{\perp} + \alpha^2 \left[\frac{\tilde{\omega}_1 + \tilde{\omega}_3}{4} + \frac{U\sqrt{\tilde{\omega}_1}}{\alpha\sqrt{2\pi}} \ln \left(\frac{16}{q^2} \frac{\Omega_{\perp}}{\alpha^2 \tilde{\omega}_1} \right) \right. \\ &\quad \left. - \frac{2\sqrt{2}}{\sqrt{\pi}} \sqrt{\frac{\tilde{\omega}_1 \tilde{\omega}_3}{\tilde{\omega}_1 + \tilde{\omega}_3}} \ln \left(\frac{8}{q^2} \frac{\Omega_{\perp}}{\alpha^2} \left(\frac{1}{\tilde{\omega}_1} + \frac{1}{\tilde{\omega}_3} \right) \right) \right].\end{aligned}\quad (44)$$

Note, that the second term in the right-hand side of Eq. (44) is proportional to α^2 , as is expected in the strong coupling regime. When replacing $\Omega_{\perp} \rightarrow \omega_c$ at $q = 2$, this polaronic term coincides with that of the bipolaron variational energy in a strong magnetic field from Ref. [29]. The dependence of the bipolaron binding energy on the cylindrical confinement provides a possibility for a controllable enhancement of the bipolaron binding by decreasing the radius of a quantum wire.

Setting $U = 0$ and $\tilde{\omega} = \tilde{\omega}_1 = \tilde{\omega}_3$ in Eq. (44), one obtains the twice variational polaron energy $2E_p$ with the variational parameter $\tilde{\omega}$ (see Ref. [25]). The polaron energy E_p depends on the confinement parameter similarly to E_{bip} . The binding energy W (which is not written explicitly to save space) increases logarithmically with increasing Ω_{\perp} .

IV. DISCUSSION OF NUMERICAL RESULTS

Beyond the framework of the limiting cases which allow an analytical treatment as discussed above, the bipolaron stability is studied using the following computational procedure.

First, we evaluate the bipolaron energy E_{bip} and the model bipolaron effective mass defined as $m_{\text{bip}} = 2(M_{\parallel} + m)$. Second, the functions $\alpha_{\text{min}}(R)$ and $\eta_c(\alpha, R)$ are found from Eq. (3). The region of the Fröhlich coupling constant ranging from 2 to 4 is chosen for the numerical work in order to include the values of α corresponding to some specific substances with small η (for example, TiO_2 : $\alpha = 2.03$, $\eta = 0.035$ [30]; TlCl : $\alpha = 2.56$, $\eta = 0.133$ [31]; BaO : $\alpha = 3.23$, $\eta = 0.118$ [30]; LiBr : $\alpha = 4.15$, $\eta = 0.24$ [31]).

Fig. 3 illustrates the size dependence of the bipolaron binding energy in cylindrical and planar quantum wires, for α values corresponding to the above-mentioned substances and for $\eta = 0$. As seen from Fig. 3, the bipolaron binding energy monotonously rises with increasing transverse confinement [cf. Eqs. (24) to (30)].

In Fig. 4, the minimal value α_{min} is represented as a function of R and L for cylindrical and planar quantum wires, correspondingly. In the region of large R and L , the minimal values α_{min} for cylindrical and planar quantum wires tend to the three-dimensional and two-dimensional limits $\alpha_{\text{min},3\text{D}}$ and $\alpha_{\text{min},2\text{D}}$, respectively. When R and L decrease from 1.0 to 0.1, a rapid diminution of α_{min} is seen. Note that at small values of R, L (which are, however, still compatible with the continuum description), the bipolaron stability region extends to small values of α . Note that the bipolaron parameters for quantum wires obtained in the formal limiting cases $R, L \rightarrow 0$ differ substantially from those derived for the purely one-dimensional model [18] (with 1D-electrons and 1D-phonons), which gives $\alpha_{\text{min},1\text{D}} = 0.9$.

In Fig. 5, the ratio of the critical value of the Coulomb repulsion constant to the Fröhlich coupling constant α ,

$$\frac{U_c(\alpha)}{\alpha} = \frac{\sqrt{2}}{1 - \eta_c(\alpha)} \quad (45)$$

is plotted as a function of α for various radii (ranging from 0.01 to 20.0) of the cylindrical quantum wire. Since the parameter η_c is non-negative, $U_c(\alpha)/\alpha$ cannot be less than the value $\sqrt{2}$ (shown by the line *A*). When increasing α , the right-hand side of Eq. (45) tends to the three-dimensional limit $\sqrt{2}/(1 - \eta_{c,3\text{D}})$, marked by the line *B*. The physical sense of this trend consists in the following: when increasing the electron-phonon coupling, the electron confinement to the *parabolic potential* (8) is gradually replaced by the confinement to the *polaronic potential* well. The regions of bipolaron stability can exist only between the lines *A* and *B*. The domain between a curve $U_c(\alpha)/\alpha$ and the line *A* is the bipolaron stability region for a specific radius of the cylindrical quantum wire. This figure illustrates clearly an enlargement of the bipolaron stability region with decreasing the radius of the quantum wire. An analogous dependence of the bipolaron stability region on the width takes place for the planar quantum wire.

Bipolaron effective masses are represented in Fig. 6 as a function of the dimensionless sizes R and L of the cylindrical and planar quantum wires. The size dependence of the bipolaron effective mass is qualitatively similar to that of the ground state energy but appears to be substantially more pronounced. At small radii ($0.1 \leq R \leq 0.2$), the bipolaron mass strongly increases with decreasing R .

V. CONCLUSIONS

The conclusion of our analysis is that the confinement leads to an *enlargement of the bipolaron stability region* in cylindrical and planar quantum wires as compared to the corresponding regions of infinite three-dimensional and two-dimensional systems, respectively. For $R \sim 1$ or $L \sim 1$, the critical values α_c required for bipolaron stability are close to those for TiO_2 , TlCl , BaO and LiBr . For example, according to Fig. 4b, the bipolaron stability region sets in at the width L of the planar quantum wire of about 8 nm for parameters of TlCl . In this view, manifestations of the bipolaron phenomena might be observed in the technically achievable planar quantum wire structures.

The performed analytical and numerical analysis of the influence of confinement on the bipolaron binding energy has shown that stable bipolaron states are possible even for intermediate values of α ($\alpha \sim 2$) and for not too small values of η ($\eta \sim 0.1$) in nanostructures whose sizes are of the same order as the polaron radius R_p . Among the considered systems, the most favorable conditions for the bipolaron stability take place in planar quantum wires, where the binding energy W increases monotonously (logarithmically) with strengthening confinement. Nanostructures, whose sizes satisfy the conditions of the bipolaron stability, seem to be achievable for the modern technology.

ACKNOWLEDGMENTS

We thank V. N. Gladilin for valuable discussions. This work has been supported by the Interuniversitaire Attractiepolen — Belgische Staat, Diensten van de Eerste Minister — Wetenschappelijke, technische en culturele Aangelegenheden; Bijzonder Onderzoeksfonds (BOF) NOI of the Universiteit Antwerpen; PHANTOMS Research Network; F.W.O.-V. projects Nos. G.0287.95 and the W.O.G. WO.025.99N (Belgium). S.N.K. acknowledges a financial support from the UIA. E.P.P, S.N.K. and S.N.B. acknowledge with gratitude the kind hospitality during their visits to the UIA in the framework of the common research project supported by PHANTOMS.

REFERENCES

- ^a Permanent address: Laboratory of Multilayer Structure Physics, Department of Theoretical Physics, State University of Moldova, str. A. Mateevici, 60, MD-2009 Kishinev, Republic of Moldova. Also at: Technische Universiteit Eindhoven, P. O. Box 513, 5600 MB Eindhoven, The Netherlands.
- ^b Also at: Universiteit Antwerpen (RUCA), Groenenborgerlaan 171, B-2020 Antwerpen, Belgium and Technische Universiteit Eindhoven, P. O. Box 513, 5600 MB Eindhoven, The Netherlands.
- ^c Present address: Theoretische Fysica van de Vaste Stof, Departement Natuurkunde, Universiteit Antwerpen (U.I.A.), Universiteitsplein 1, B-2610 Antwerpen, Belgium.
- [1] L. D. Landau, *Phys. Z. Sowjetunion* **3**, 664 (1933) [in Russian; English translation in: *Collected Papers* (Gordon and Breach, New York, 1965), pp. 67—68].
- [2] S. I. Pekar, *Research on Electron Theory in Crystals* (Gostekhteorizdat, Moscow and Leningrad, 1951) [in Russian; English translation: US AEC, Washington DC, 1963].
- [3] V. L. Vinetskii and M. S. Giterman, *Zh. Eksp. Teor. Fiz.* **33**, 730 (1957).
- [4] V. K. Mukhomorov, *Fiz. Tekh. Poluprovodnikov* **16**, 1095 (1982) [*Sov. Phys.—Semicond.* **16**, 799 (1982)].
- [5] S. G. Suprun and B. Ya. Moizhes, *Fiz. Tverd. Tela* **24**, 1571 (1982) [*Sov. Phys.—Solid State* **24**, 903 (1982)].
- [6] V. L. Vinetskii, O. Meredov, and V. A. Yanchuk, *Teor. Exp. Khim.* **25**, 641 (1989).
- [7] J. Adamowski, *Acta Phys. Pol. A* **73**, 345 (1988); *Phys. Rev. B* **39**, 3649 (1985).
- [8] S. Sil, A. K. Giri, and A. Chatterjee, *Phys. Rev. B* **43**, 12642 (1991).
- [9] N. I. Kashirina, E. V. Mozdor, E. A. Pashitskii, and V. I. Sheka, *Izvestiya Akademii Nauk SSSR, Ser. Fizicheskaya* **59**, 127 (1995).
- [10] J. T. Devreese, in: *Encyclopedia of Applied Physics* (VCH Publishers, Weinheim, 1996), **14**, pp. 383—413.
- [11] F. M. Peeters and J. T. Devreese, *Phys. Rev. B* **31**, 4890 (1985).
- [12] R. R. Hudgins, P. Durourd, J. M. Tenenbaum, and M. F. Jarrold, *Phys. Rev. Lett.* **78**, 4213 (1997).
- [13] G. Verbist, F. M. Peeters, and J. T. Devreese, *Solid State Commun.* **76**, 1005 (1990).
- [14] G. Verbist, F. M. Peeters, and J. T. Devreese, *Phys. Rev. B* **43**, 2712 (1991).
- [15] G. Verbist, M. A. Smondyrev, F. M. Peeters, and J. T. Devreese, *Phys. Rev. B* **45**, 5262 (1992).
- [16] P. Vansant, M. A. Smondyrev, F. M. Peeters, and J. T. Devreese, *J. Phys. A: Math. Gen.* **27**, 7925 (1994).
- [17] F. Luczak, F. Brosens, and J. T. Devreese, *Phys. Rev. B* **52**, 12743 (1995).
- [18] P. Vansant, F. M. Peeters, M. A. Smondyrev, and J. T. Devreese, *Phys. Rev. B* **50**, 12524 (1994).
- [19] E. P. Pokatilov, S. I. Beril, V. M. Fomin, and G. Yu. Ryabukhin, *Phys. Stat. Sol. (b)* **169**, 429 (1992).
- [20] E. P. Pokatilov, S. I. Beril, V. M. Fomin, G. Yu. Ryabukhin, and G. R. Goryachkovskii, *Phys. Stat. Sol. (b)* **171**, 437 (1992).
- [21] E. P. Pokatilov, V. M. Fomin, J. T. Devreese, S. N. Balaban, S. N. Klimin, and L. C. Fai, *Superlattices and Microstructures* **23**, 331 (1998).
- [22] S. N. Klimin, E. P. Pokatilov, and V. M. Fomin, *Phys. Stat. Sol. (b)* **184**, 373 (1994).

- [23] L. Wendler, A. V. Chaplik, R. Haupt, and O. Hipolito, *J. Phys.: Condensed Matter* **5**, 4817 (1993).
- [24] S. Sahoo, *Z. Phys. B* **101**, 97 (1996).
- [25] E. P. Pokatilov, V. M. Fomin, J. T. Devreese, S. N. Balaban, and S. N. Klimin, *Physica E* **4**, 156 (1999).
- [26] R. P. Feynman, *Phys. Rev.* **97**, 660 (1955).
- [27] R. P. Feynman and A. R. Hibbs, *Quantum mechanics and path integrals* (McGraw-Hill, New York, 1965).
- [28] M. A. Smondyrev, J. T. Devreese, and F. M. Peeters, *Phys. Rev. B* **51**, 15008 (1995).
- [29] F. Brosens and J. T. Devreese, *Solid State Commun.* **96**, 133; 619 (1995); *Phys. Rev. B* **54**, 9792 (1996).
- [30] Yu. A. Firsov (ed.), *Polarons* (Nauka, Moscow, 1975) [in Russian].
- [31] E. Kartheuser, in: J. T. Devreese (Ed.), *Polarons in Ionic Crystals and Polar Semiconductors* (North-Holland, Amsterdam, 1972), pp. 717-733.

FIGURE CAPTIONS

Fig. 1. A scheme of the trial system which contains two electrons connected with two “fictitious” particles through the elastic attraction and models the Coulomb interaction by the elastic repulsion.

Fig. 2. A scheme of cylindrical (a) and planar (b) quantum wires.

Fig. 3. The bipolaron binding energy W in cylindrical (a) and planar (b) quantum wires plotted versus the dimensionless radius R and width L , respectively.

Fig. 4. The minimal value (at $\eta = 0$) of the critical electron-phonon coupling constant α_c plotted versus R and L in cylindrical (a) and planar (b) quantum wires, respectively.

Fig. 5. The ratio of the critical Coulomb repulsion constant U_c and α , as a function of α , in cylindrical quantum wires for $R = 0.01$ (1), 0.5 (2), 1.0 (3), and 20.0 (4).

Fig. 6. The bipolaron effective mass $(m_{\text{bip}})_{\parallel}/m$ in cylindrical (a) and planar (b) quantum wires plotted versus R and L , respectively. The curves for the effective mass are broken off as the bipolaron becomes unstable.

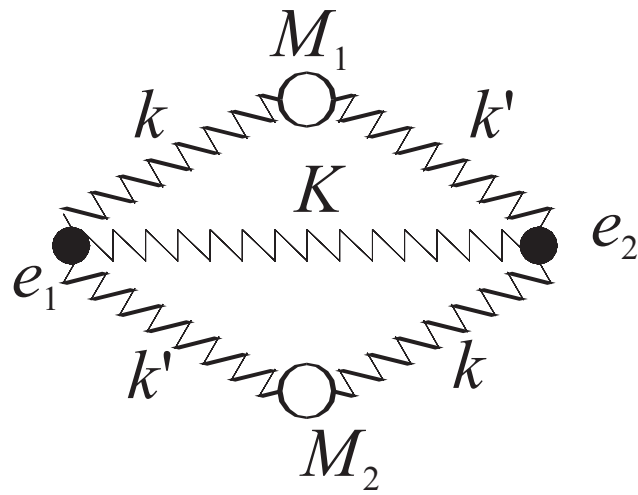


Fig. 1. A scheme of the trial system which contains two electrons connected with two “fictitious” particles through the elastic attraction and models the Coulomb interaction by the elastic repulsion.

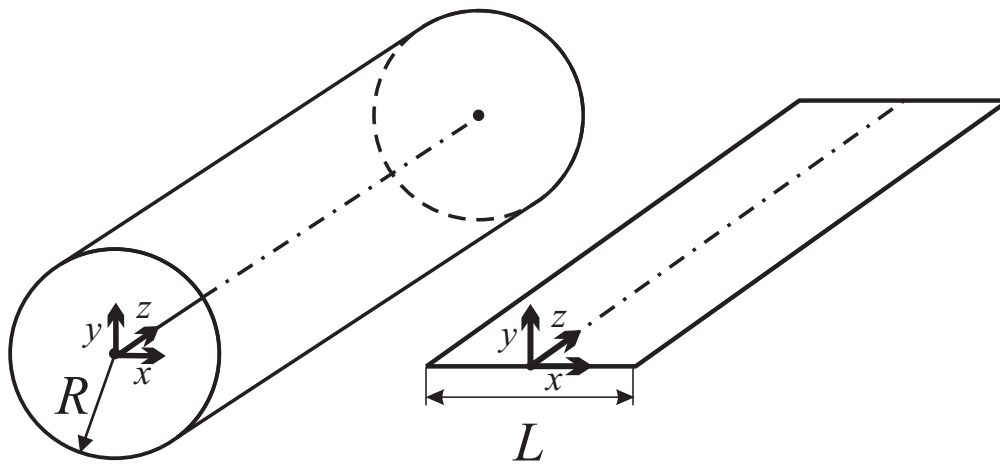


Fig. 2. A scheme of cylindrical and planar quantum wires.

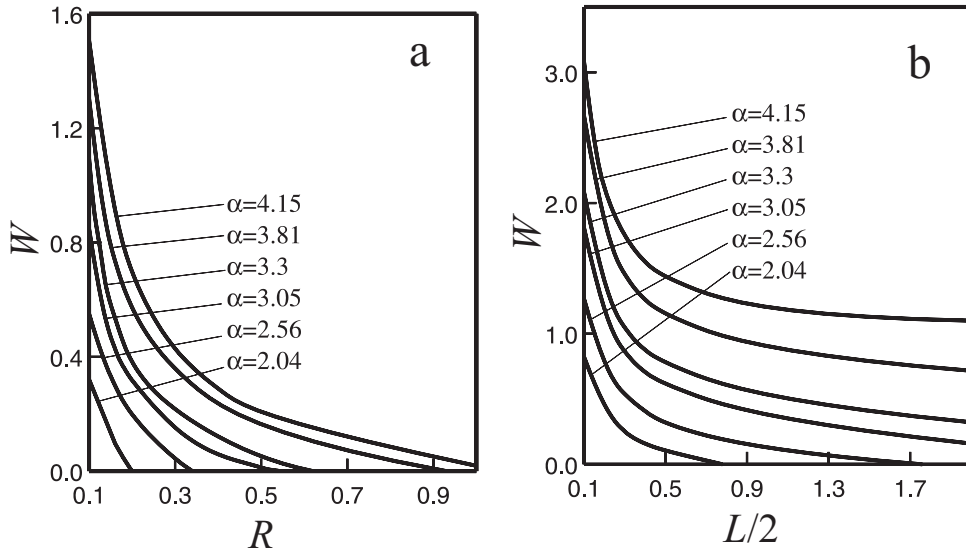


Fig. 3. The bipolaron binding energy W in cylindrical (a) and planar (b) quantum wires plotted versus the dimensionless radius R and width L , respectively.

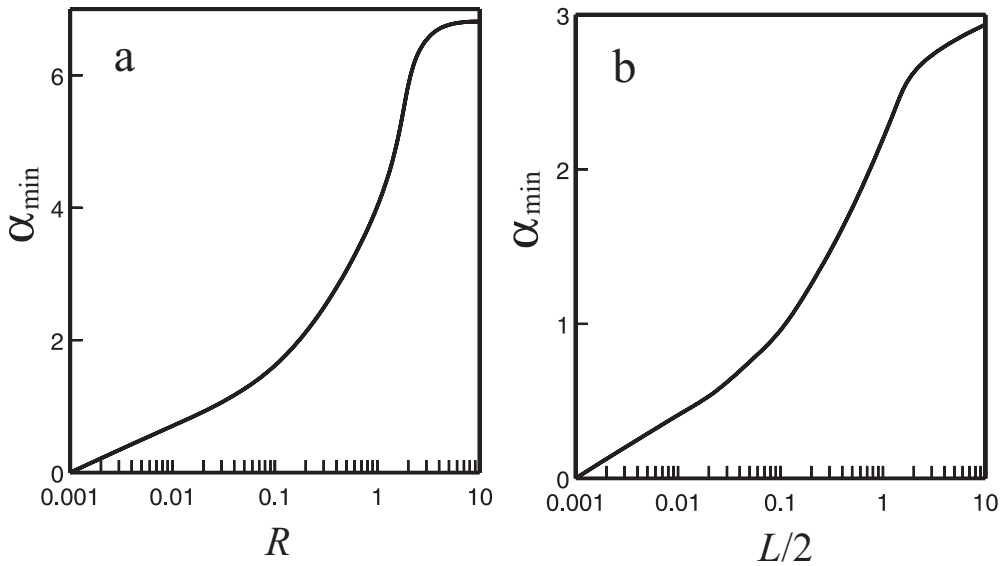


Fig. 4. The minimal value (at $\eta=0$) of the critical electron-phonon coupling constant α_c plotted versus R and L in cylindrical (a) and planar (b) quantum wires, respectively.

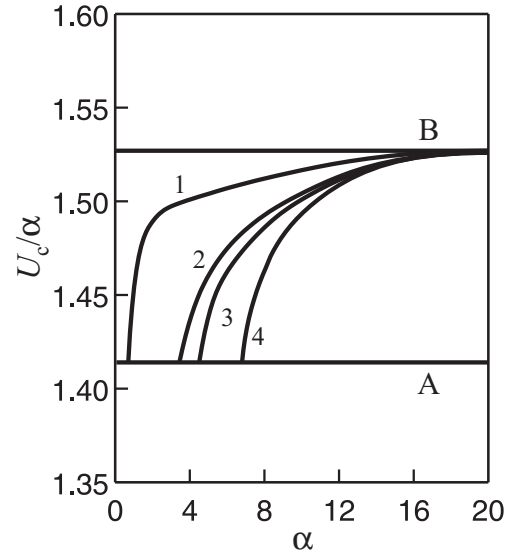


Fig. 5. The ratio of the critical Coulomb repulsion constant U_c and α , as a function of α , in cylindrical quantum wires for $R=0.01$ (1), 0.5 (2), 1.0 (3), and 20.0 (4).

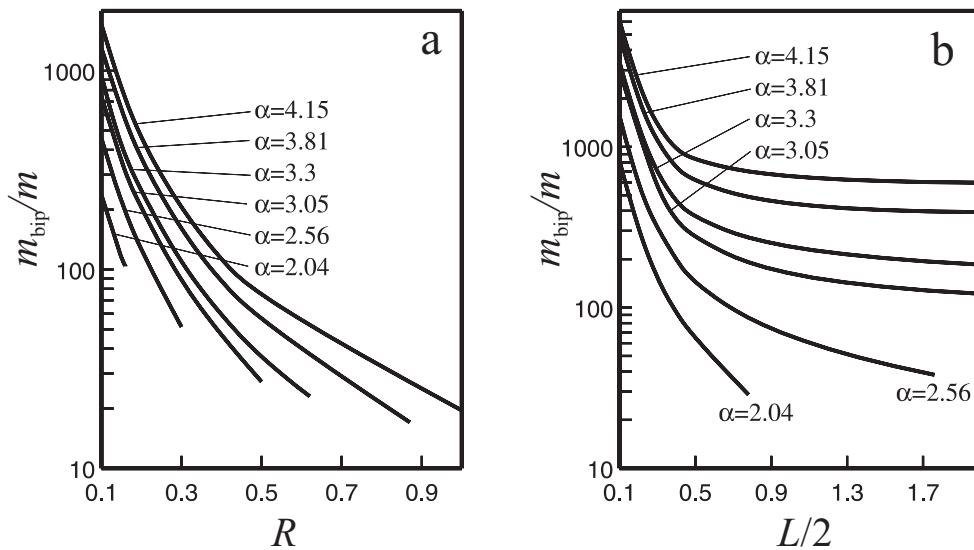


Fig. 6. The bipolaron effective mass m_{bip}/m in cylindrical (a) and planar (b) quantum wires plotted versus R and L , respectively. The curves for the effective mass are broken off as the bipolaron becomes unstable.